SLAC-TN-07-028

Measurements of High-Field THz Induced Photocurrents in Semiconductors

Michael Wiczer

Office of Science, SULI Program

University of Illinois – Urbana-Champaign

Stanford Linear Accelerator Center

Stanford, CA

August 24, 2007

Prepared in partial fulfillment of the requirements of the Office of Science, Department of Energy's Science Undergraduate Laboratory Internship under the direction of A. M. Lindenberg in the Stanford Synchrotron Radiation Laboratory at the Stanford Linear Accelerator Center.

Participant: _____
Signature

Research Advisor: _____
Signature

Work supported in part by US Department of Energy contract DE-AC02-76SF00515

Table of Contents

Abstract

Measurements of High-Field THz Induced Photocurrents in Semiconductors. MICHAEL WICZER (University of Illinois – Urbana-Champaign, Urbana, IL 61801) AARON LINDENBERG (Stanford Linear Accelerator Center, Menlo Park, CA 94025).

THz pulses have provided a useful tool for probing, with time resolution, the free carriers in a system. The development of methods to produce intense THz radiation has been slow since spectroscopists and condensed matter physicists first began probing materials with THz pulses. We have developed a method for producing intense ultra-short THz pulses, which have full width half maximum of 300 fs – approximately a half cycle of THz radiation. These intense half cycle pulses (HCPs) allow us to use THz radiation not only as a probe of the free carriers in a system but also as a source of excitation to alter a system in some way. In particular, HPCs perturb free carriers considerably in short time scales but show minimal effect to individual free carriers over long time. By exposing the semiconductor indium antimonide (InSb) to our intense THz HCP radiation, we have observed non-linear optical effects which suggest the generation of new free carriers by below band-gap THz photons. This generation of free carriers appears to be caused by an avalanche multiplication process, which should amplify the number of free carriers already in the system and then induce a current in the timescale of our THz pulse. This amplification on such a short timescale suggests the possibility of an ultra-fast detector of weak above band-gap radiation. We constructed a device which detects these currents by painting an electrode structure on the surface of the semiconductor. The currents induced across the electrodes by this avalanche multiplication process were measured and compared with other measurements of this non-linear optical process. We successfully measured THz induced currents in InSb, which indicate promise towards the development of an ultra-fast detector, and

we gain insight into a possible physical explanation of the THz induced free carriers we observe in InSb.

Introduction

Ultra-fast THz (10^{12} Hz) radiation has proved tremendously useful for probing time-resolved dynamics in a variety of systems [1]. Traditionally, a sample is excited or set into motion in some way (i.e. by a "pump" such as an IR-laser pulse or synchrotron radiation pulse) and at various times following this excitation, a THz pulse passes through the sample and "probes" its state at that instant. THz radiation is an extremely good probe of systems because each THz photon has very low energy (1 THz photon ~ 4 meV). Thus, the radiation is absorbed by free electrons in the system (a detectable effect), but the small increase in the energy of the free electron has no discernible effect on the system. Although this has been a powerful tool for studying dynamics for some time, we are beginning to learn that – at high enough intensity – THz radiation can act as a valuable source of excitation ("pump") of a system.

New techniques have provided for the generation of THz radiation by optical rectification [2] not limited in intensity by a threshold for damaging a non-linear optical crystal. We have developed an experimental setup which uses a plasma in air as a nonlinear optical element. For our purposes, the THz radiation generated by this method is only limited by the intensity of incident 800 nm and 400 nm laser light. With this tool available, we can begin to study ultra-fast dynamics using THz radiation as a pump.

One such experiment employing this high intensity THz radiation studies its interaction with semiconductors. Indium antimonide (InSb) was placed in the path of the THz beam and absorption was measured. Since the photons had much lower energy than the band-gap of the semiconductor (4 meV << .17 eV), one would not expect the THz radiation to increase the

number of free carriers in the semiconductor. Instead, the THz absorption should provide a measure of the number of free carriers currently present in the semiconductor (due to thermal excitation). However, we have observed that THz radiation at high enough intensity generates new free carriers. We measure this phenomenon by using the THz pulse as a probe of its own interactions and by observing current generated by the new free carriers.

Our THz radiation is short enough (~300 fs FWHM) to be considered a half-cycle pulse [3]. In this case, the integral of electric (or magnetic) field over all time is 0, but one half-cycle of the electric field is much stronger than all others (Figure 1). Thus, for short times, the THz pulse can act as a positive field. If this field is strong enough, it can accelerate existing free carriers in the conduction band of the semiconductor. Once accelerated, these free electrons can collide with valence electrons, and, if there is enough energy, create new electron-hole pairs. The new conduction band electrons can now feel the electric field and accelerate into valence electrons to produce even more electron-hole pairs [4-6]. Upon investigating this process – avalanche multiplication – we observe that the ultra-fast, high intensity THz radiation provides for an experiment which isolates certain physical processes extremely well. While in bulk systems, electron-electron collisions in the conduction band and electron-phonon coupling prove significant, both of these processes occur on much longer time-scales than our experiment. Furthermore, fields this intense are generally unable to penetrate the surface of the semiconductor material, which breaks down at much lower fields. The ultra-fast nature of the pulse once again allows for the pulse to excite the sample before it breaks down, and the field is not screened.

This setup may assist the development of an ultra-fast detector. Our THz radiation can multiply the number of free carriers in the semiconductor and produce a current in very short

timescales. This amplification can be harnessed by the construction of a photoconductive dipole antenna [7-8]. By placing two electrodes on the surface of the sample with the polarization of the THz beam pointing across the electrodes, the THz beam will sweep and multiply any newly generated free carriers (i.e. by an above band-gap photon). This device, which generally uses a known pulsed laser to detect small THz signals, can use a known THz signal to detect small laser signals with high gain and very fast response – as fast as the THz pulse length. As yet, no detection method this fast exists.

Materials and Methods

We generate high-intensity THz pulses with a Ti:Sapphire laser system. A mode-locked Ti:Sapphire oscillator produces weak, 25 fs pulses, which are then sent to a regenerative amplifier to be amplified using chirped pulse amplification (CPA) [9]. The final laser pulses have total energy of approximately 1 mJ, pulse length of 50 fs, wavelength centered at 800 nm (full width half maximum spanning from about 775-825 nm), and a repetition rate of 1 KHz. These laser pulses are then passed through a β-barium borate (BBO) frequency-doubling crystal to produce 400 nm light collinear with the original 800 nm light. As described by Bartel et al, if this beam is focused to a small enough waist to ionize air – and has an appropriate divergence angle for optimal phase matching – a 3-rd order non-linear optical effect will produce a quasi-DC electromagnetic field. Since the pulse duration for the incoming laser beams are so short, this quasi-DC field takes the form of an ultra-short THz pulse [10].

A sample photoconductive antenna is constructed in order to test both the physics of the interaction between intense THz radiation and semiconductor samples as well as the potential development of an ultra-fast photoconductive switch. Using silver paste two vertical electrodes, approximately 5 mm in length and separated by 500 μm, were painted onto the InSb sample.

Although InSb is a semiconductor, its extremely narrow band-gap allows for a high density of free carriers even at room temperature ($2\times10^{16}\ cm^{-3}$). Thus, it has a relatively low resistivity, and the resistance across the two electrodes was measured to be approximately 50 Ω. Since the heat of a soldering iron damages the semiconductor material, wires were attached to the surface of the semiconductor with epoxy, and electrical contact with the electrodes was ensured with additional silver paste. In order to minimize the amplification of ambient electrical noise, wire directly from a coaxial cable was mounted to the sample and cable length was minimized (Figure 2). The current across these electrodes was input into a current amplifier (Stanford Research Systems SR570) set to a gain of 1 pA/V. This was the most sensitive gain setting on the current amplifier, and thus the output from the amplifier was slow (output time constant of 3.5 s). An optical shutter (Thorlabs SH05 shutter with Thorlabs SC10 controller) modulated the beam at .2 Hz. A reference signal from this shutter and the output of the current amplifier were synchronized using a lock-in amplifier (SR830) acquiring with a time constant of 100 s.

This type of device has been used extensively in the past to detect THz radiation [7]. When used with a semiconductor with carrier lifetimes of approximately or less than the width of the THz pulse, the current induced across the electrodes increases linearly with electric field amplitude for low fields. If the carrier lifetimes are much longer than the width of the THz pulse (as in InSb) and no new free carriers are induced, a free carrier feels the electric field of the THz pulse for a very long time, and the current across the electrodes is approximately zero. If, however, new free carriers are induced, then the average conduction band electron loses energy at every collision. The electron no longer feels the electric field uninterrupted for the entire width of the pulse. Rather during the positive portion of the pulse, the energy decreases. The now slower free carrier then feels the rest of the field, which reduces its velocity further until the net

velocity of free carriers is in the direction opposite the direction the charge was accelerated during the THz pulse. This results in a net current indicative only of the free carriers generated during the positive portion of the THz pulse (Figure 3). The expectation at high THz intensity is that, once the field reaches an impact-ionization threshold, additional free carriers will be generated, and a current will form. We measure the dependence of current on incident electric field by focusing our THz beam to a small waist and translating the sample along the direction of propagation of the THz beam. At the beam waist, the electric field amplitude will be greatest and as the sample is translated away from the waist, the amplitude decreases.

The intention is that we acquire data as the photoconductive antenna translates along the propagation axis of the focusing THz beam. This data then needs to be calibrated to be expressed against peak electric field instead of position. To this end, we mapped the THz beam as it propagates. We use a bolometer, which measures the total THz intensity incident on the detector. Spatial resolution is provided by blocking all THz radiation except that which passes through a narrow slit (Figure 4). The slit is open to a small portion of the THz beam's longitudinal profile at a particular propagation distance; the THz intensity incident on the bolometer is a measure of the THz intensity at the position of the slit.

Results

Modeling:

In order to characterize the physical processes involved in our experiment, we must produce a model which predicts a signature of the suspected physical process, which might be measurable. We produce a simple "order-of-magnitude" model for the current generated by avalanche multiplication induced by THz radiation in InSb. Since the THz wavelength is so long and the pulses so intense, it is an accurate picture to consider the effect of the bulk electric field

created by the THz radiation as opposed to multi-photon absorption – which is a much more complex description of the process. The traditional treatment of semiconductors exposed to fields as high as the peak field of the THz HCP we generate (approximately 200 KV/cm) is to suggest that a free electron reaches a saturation velocity because of the increased number of collisions at fields this high. Furthermore, avalanche breakdown will occur, the semiconductor will become a conductor, and fields will be screened. However, the THz pulses we generate are short enough that relatively few collisions occur. Hence, the electron can – for this short duration – transport through the semiconductor at velocities much greater than the saturation velocity, and fields much greater than the breakdown field of the semiconductor can penetrate the sample. Thus, a "hot-electron" transport model – one where the electron has a fixed energy incident on the material – appears more appropriate than a high-field transport model – one where the electron starts at rest and then is accelerated. Kane developed a model for the rate of impact ionization collisions – collisions with valence electrons which create new electron-hole pairs – as a function of a hot electron's kinetic energy [4]. Based on Kane's "random-k" approximation, we find that – if the hole effective mass is much greater than the free carrier effective mass – the collision rate, ω(E), is related to the following integral expression [4]:

$$\omega(E_1) \propto \int_{E_g}^{E_1-E_g} \int_{E_g}^{E_1-E_3} \varphi_c(E_2)\varphi_c(E_3)\varphi_v(E_4)dE_2dE_3$$

Where E_1 is the energy of the initial hot electron and E_4 is the energy of the valence electron which interacts with the initial hot electron. Once the hot electron interacts with the valence electron, the hot electron loses energy and the valence electron gains enough energy to enter the conduction band. This produces two final electrons in the conduction band with energies E_2 and E_3. The conservation of energy condition is that $E_1=E_2+E_3-E_4$. All energies are measured from

the valence band edge, and the band gap energy is E_g (E_g = 0.17 eV for InSb (E_4<0; E_1,E_2,E_3>E_g). φ_c is the density of states function of the conduction band and φ_v is the density of states for the valence band. If we assume a parabolic band structure, these functions become

$$\varphi_c(E) = \frac{1}{2\pi^2}\left(\frac{2m_c}{\hbar^2}\right)^{3/2}\sqrt{E-E_g}\,,\ \varphi_v(E) = \frac{1}{2\pi^2}\left(\frac{2m_v}{\hbar^2}\right)^{3/2}\sqrt{-E}$$

Where m_c is the effective mass of a free electron (0.014 m_e in InSb) and m_v is the effective mass of a hole (0.43 m_e in InSb). This integral was evaluated and the constant of proportionality was determined by calibrating our results to previous Monte-Carlo calculations of low-energy impact ionization rates in InSb [5]. The calculated collision rate is given in Figure 5.

Using this, we must now consider that the electron, in fact, starts at rest and is accelerated. The instantaneous collision probability per unit time, P(t), must satisfy

$$P(t) = \left(1 - \int_{t_0}^{t} P(s)ds\right)\omega\big(E(t)\big)$$

Where t_0 is the time for the electron to accelerate to the threshold energy and E(t), under a constant field, is given by $E(t) = \frac{1}{2m^*}\big(qFt\big)^2$. For various field strengths, P(t) and, in turn, the average times for the first ionizing collision were calculated. The dependence of collision time on applied field (assuming a constant field) τ(F) was found to be given by $\tau(F) \propto (F - F_t)^{-0.9}$ (Figure 6), where F_t is the threshold field for impact ionization. If we approximate our THz pulse as a square wave, we can generate an approximation for the multiplication factor:

$$M(F) = 2^{t_p/\tau(F)}$$

where t_p is the width of the pulse. It is important to note that many assumption have been made which cause considerable inaccuracies in the multiplication factor. We believe that the given

expression for the multiplication factor is nevertheless useful in understanding qualitative trends and achieving order-of-magnitude approximations.

Experiment:

Using slits to provide spatial resolution to our bolometer measurement (as described in Materials and Methods section), we acquired a map of the intensity profile of the THz beam as it propagates (Figure 7). After extracting the intensity peak at each position along the propagation axis (and then taking the square root of intensity) we were able to extract the relative peak electric field as a function of position along the propagation axis (Figure 8).

Once the THz beam profile was achieved, the electrode structure (Figure 2) was placed at the focus of the THz beam. Current was measured where the electrodes were placed at various longitudinal positions along the beam profile (Figure 9). The width of the current profile was approximately 750 μm FWHM, which is comparable to the width of the THz intensity profile at the focus. This suggests that the current measured is, in fact, induced by the THz beam. We then placed the electrode structure at various positions along the propagation axis of the THz beam (Figure 10). The current profile was much broader than the intensity profile of the THz beam. Some current was found when no THz radiation was generated but 800 nm IR radiation was incident on the electrode gap. This suggests that the current profile of the THz beam may have been broadened by scattered IR radiation.

Discussion and Conclusions

We have tentatively observed THz induced photocurrents on 300 fs timescales. The mere existence of this photocurrent is valuable as it shows promise as an ultra-fast, high gain photoconductive switch – a fast detector of weak above-band-gap radiation. Although these data have not yet been related to similar absorptions measurements, we expect that after repeating our

photocurrent measurements with improved scattered light cancellation the absorption and photocurrent measurements will relate in interesting ways.

It is valuable here to speculate about frequency dependences. The frequency response of the bolometer that was used for absorption measurements favors higher frequencies. Furthermore, in low-intensity conditions, InSb absorbs low frequency THz radiation considerably more than higher frequency THz. This suggests that our absorption measurements, which indicate an increase in free carriers, are mostly providing insight in the response of InSb to higher frequency THz radiation. Based on the impact ionization model, we understand that the width of the HCP is extremely significant to the gain generated by avalanche multiplication. Lower frequency components help to broaden the HCP. Our understanding of the photoconductive antenna, on the other hand, suggests that it can provide insight into the response of InSb to low as well as high THz frequencies. This is because the electrodes are on the surface of the sample, so absorption effects through the depth of the sample are insignificant. Furthermore, our understanding of the mechanism which generates photocurrents suggests that the current is much more sensitive to the properties of the electric field of the THz pulse as a function of time as opposed to the frequency components. The lack of frequency discrimination in the photoconductive antenna and the observation that the effects of impact ionization are amplified by the present of low frequency THz radiation suggest that the photoconductive antenna should be more sensitive to these non-linear effects than the absorption measurements. Thus, currents should begin to develop at lower peak intensity than increased absorption began. This seems to support our tentative results that the current profile is broader than the absorption profile of the THz beam. It does not change the fact that scattered IR light may have played a significant role in broadening the current profile, but a broader profile is expected nevertheless.

Necessary further investigation includes the repetition of our measurement of the photocurrent profile with the effects of scattered IR light being reduced. Furthermore, we would like to repeat our measurements at low temperatures. This will provide direct evidence for whether the non-linear effects we observe are produced by conduction band electrons or valence band electrons since, as the conduction band electrons are reduced, the effect will be either enhanced or reduced. Finally, we should refine our photoconductive antenna design for use as an ultra-fast photoconductive detector.

Acknowledgments

This research was conducted at the Stanford Linear Accelerator Center (SLAC). I thank my mentor, Professor Aaron Lindenberg, and his post-doctoral associate Haidan Wen for their direction and discussions which guided this project. I also thank the Department of Energy, Office of Science for funding my research and for organizing the Science Undergraduate Laboratory Internships (SULI) program. Finally, I would like to thank the organizers of the SULI program at SLAC.

References:

[1] C.A. Schmuttenmaer, "Exploring Dynamics in the Far-Infrared with Terahertz Spectroscopy," in Chemical Reviews, Vol. 104, 2004, pp. 1759-1779.

[2] T.J. Carrig, G. Rodriguez, T.S. Clement, A.J. Taylor, and K.R. Stewart, "Scaling of Terahertz Radiation Via Optical Rectification in Electrooptic Crystals," in Applied Physics Letters, Vol. 66, 1995, pp. 121-123.

[3] T. Bartel, P. Gall, K. Reimann, M. Woerner, and T. Elsaesser, "Generation of single-cycle THz transients with high electric-field amplitudes," in Optics Letters, Vol. 30, 2005, pp. 2805-2807.

[4] E.O. Kane, "Electron Scattering by Pair Production in Silicon", in Physical Review, Vol. 159, 1967, pp. 624-631.

[5] R.C. Curby and D.K. Ferry, “Impact Ionization in Narrow Gap Semiconductor”, in Physica Status Solidi (a), Vol. 15, pp. 319-328.

[6] S.A. Jamison and A.V. Nurmikko, “Avalanche formation and high-intensity infrared transmission limit in InAs, InSb, and $Hg_{1-x}Cd_xTe$”, in Physical Review B, Vol. 19, 5185-5193.

[7] P.R. Smith, D.H. Auston, and M.C. Nuss, “Subpicosecond Photoconducting Dipole Antennas” in IEEE Journal of Quantum Electronics, Vol. 24, 1988, pp. 255-260.

[8] M. van Exter, C. Fattinger, and D. Grischkowsky, “High-brightness terahertz beams characterized with an ultrafast detector”, in Applied Physics Letters, Vol. 55, 1989, pp. 337-339.

[9] U. Keller, G. W 'tHooft* W H. Knox, and J. E. Cunningham, “Femtosecond pulses from a continuously self-starting passively mode-locked Ti:sapphire laser” in Optics Letters, Vol. 16, 1991, pp. 1022-1024.

[10] T. Bartel, P. Gall, K. Reimann, M. Woerner, and T. Elsaesser, “Generation of single-cycle THz transients with high electric-field amplitudes” in Optics Letters, Vol. 30, 2005, pp. 2805-2807.

Figures

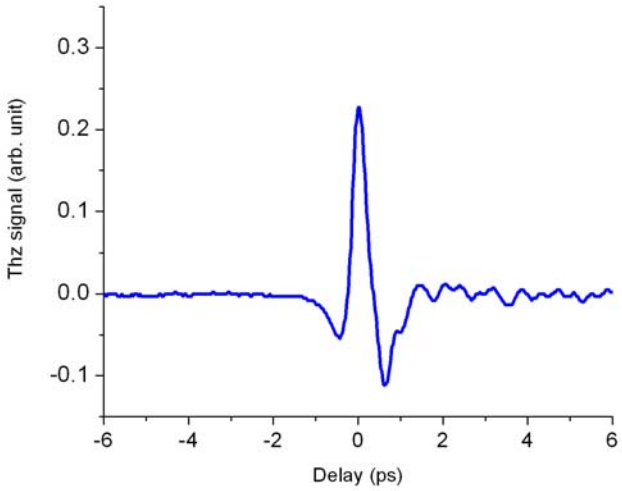

Figure 1. A half-cycle pulse of THz radiation acts as a directional electric field for short times.

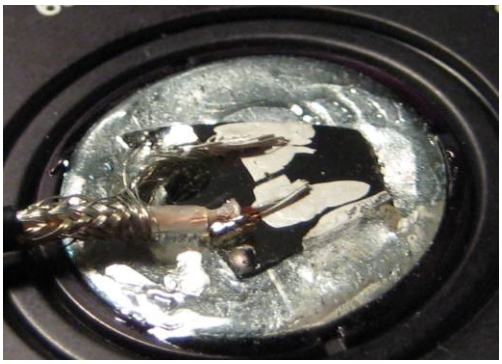

Figure 2. Electrodes attached to InSb surface with silver paint and epoxy glue.

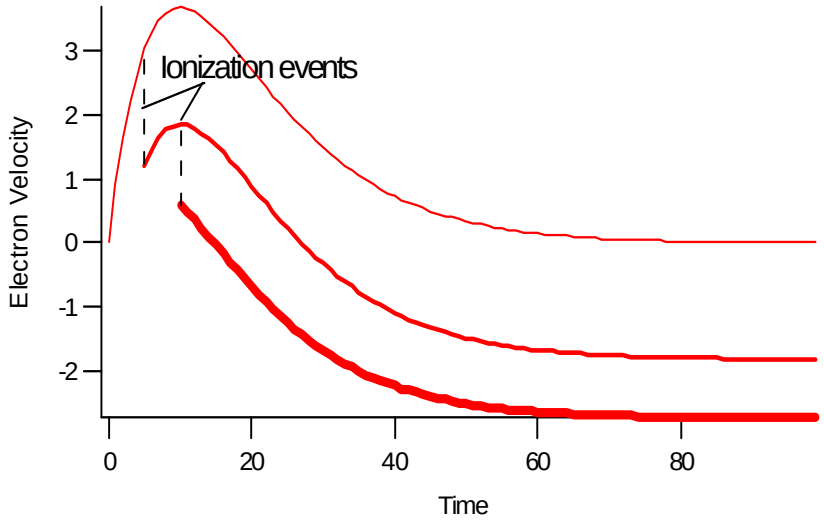

Figure 3. A free electron which is subject to a THz HCP for long times has velocity qualitatively depicted in thee top trace. For every ionization event, not only are total free carriers doubled, but the net velocity after long times becomes non-zero (bottom two traces).

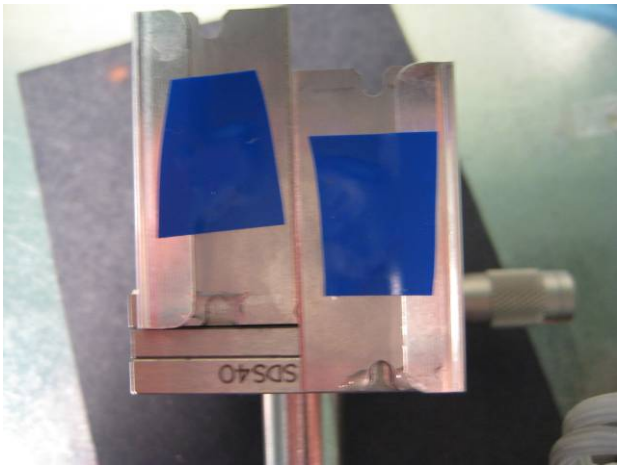

Figure 4. Width between narrow slits is adjusted by micrometer position. Only THz radiation at a specified position reaches the bolometer when the slits are positioned in front of the THz beam.

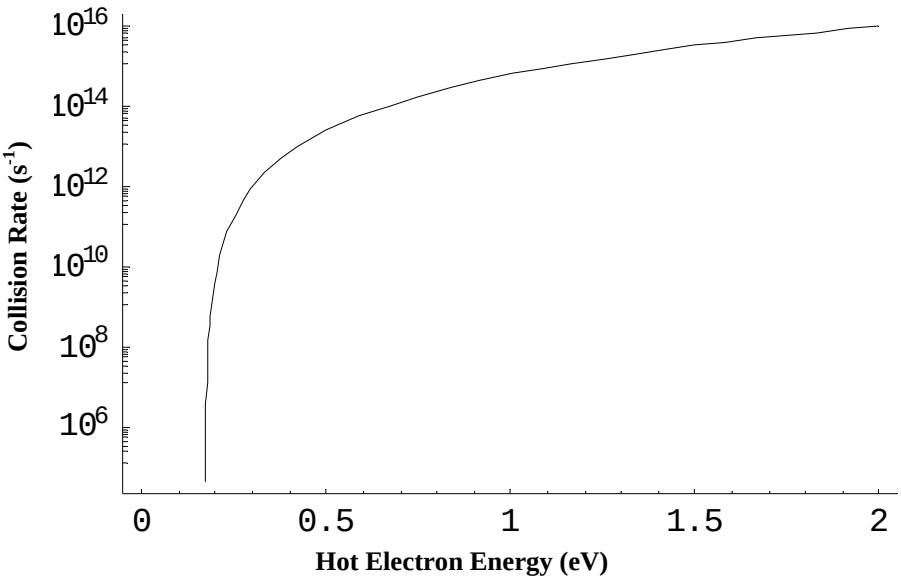

Figure 5. Probability of ionizing collision per unit time vs. electron kinetic energy.

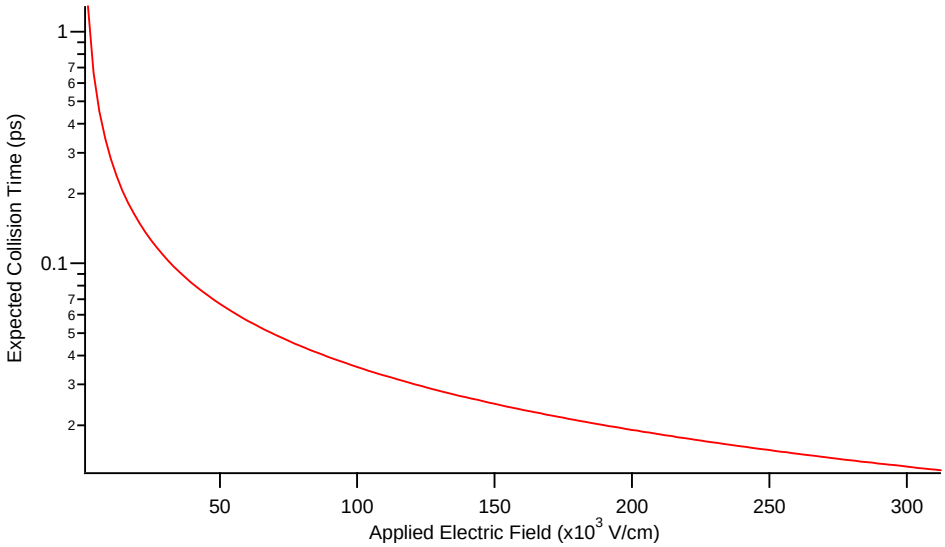

Figure 6. Expected time for first ionizing collision vs. applied field.

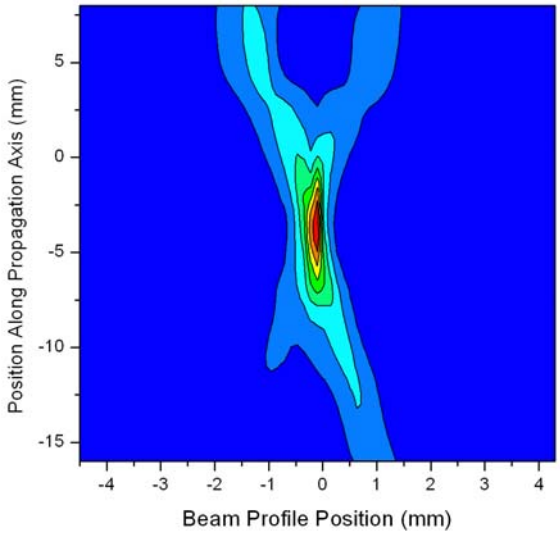

Figure 7. THz beam intensity contour plot.

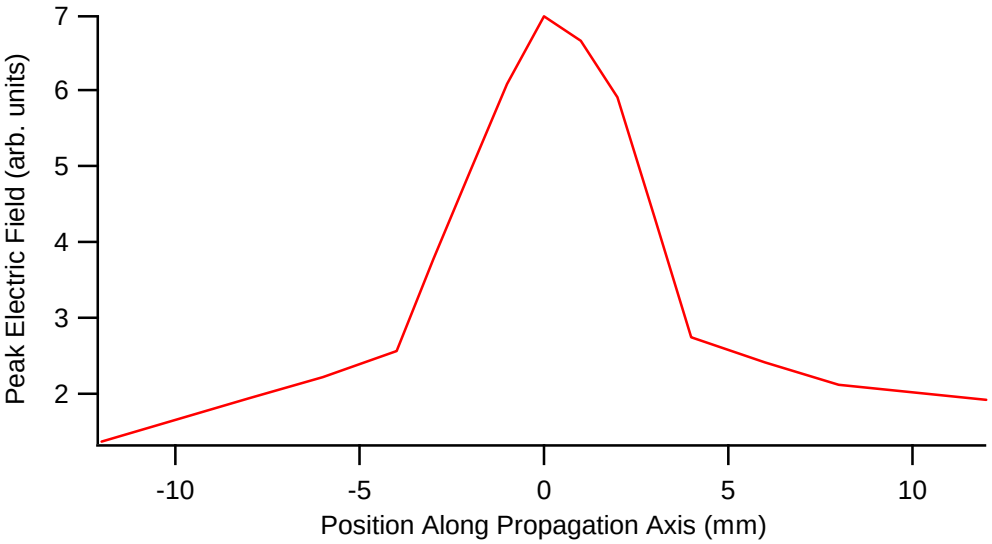

Figure 8. Peak THz electric field vs. propagation distance as beam is focused.

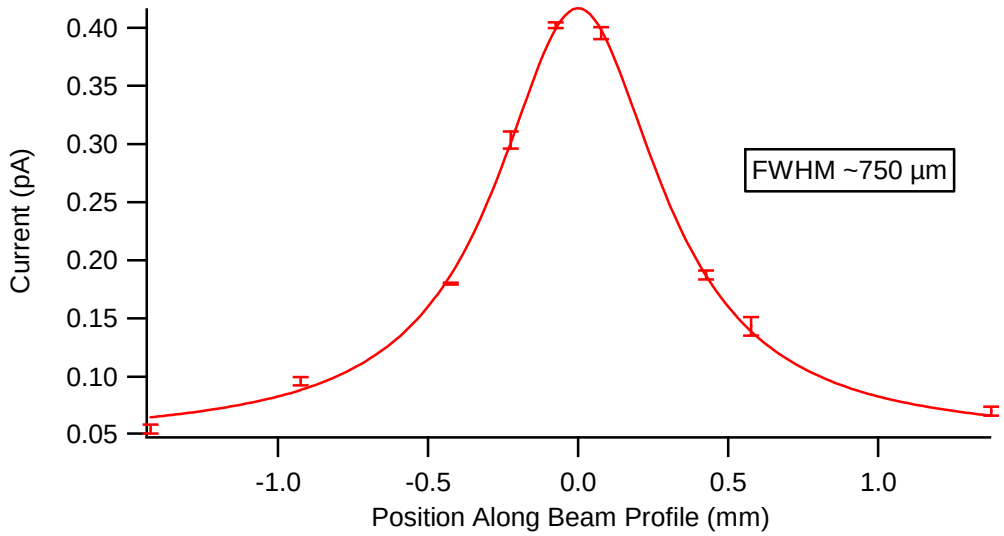

Figure 9. THz induced current vs. position along beam profile at focus of THz beam.

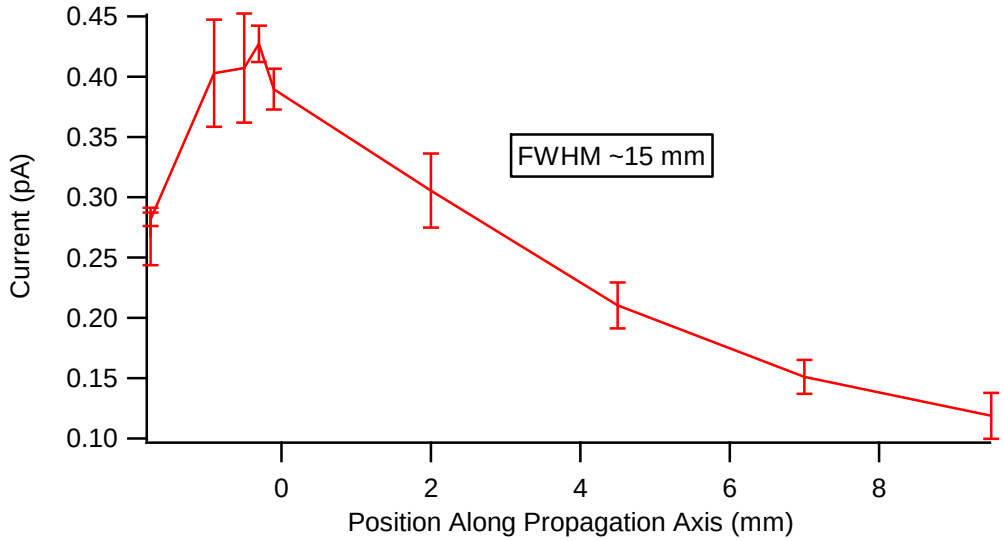

Figure 10. THz induced current vs. propagation distance as beam is focused. This trace is about twice as broad as the non-linear features observed in absorption measurements.